LOCALIZATION OF CROP DAMAGES UTILIZING A WAKE-UP GAS SENSOR NETWORK

Seungbeom Noh[1], Sayali Tope[1], Farhan Sadik Sium[1], Shakir-ul Haque Khan[1], Mohit Karkhanis[1], Leo Wang[1], Adwait Deshpande[1], Rana Dalapati[2], Ravi V. Mural[3], Carlos H. Mastrangelo[1], Mingyu Ji[1], Ling Zang[2], James C. Schnable[3], and Hanseup Kim[1]

[1]Electrical and Computer Engineering, University of Utah, Salt Lake City, UT 84112
[2]Materials Science and Engineering, University of Utah, Salt Lake City, UT 84112
[3]Department of Agronomy and Horticulture,, University of Nebraska, Lincoln, NE 68588

ABSTRACT

This paper reports the initial demonstration of on-field crop damage prediction through a network of low power gas sensors that were deployed in an actual sorghum field and detected crop stress molecules, specifically hexanal. Such detection could replace current farm-scouting methods that are mostly manual and help reduce production loss of biofuel crops during a farming period. The initially-deployed gas sensor network consisted of a 2×3 array with a 7-meter interspace. When the leaves of sorghums were cut at a random location within the network, three sensors in the gas sensor network responded at 45, 62, and 72 minutes, respectively, allowing us to estimate an origination zone within an area of 21.7 m^2 out of the total monitoring farm area of 294 m^2. This demonstration proves the potential of precise localization of plant damages through the use of the gas sensor network.

KEYWORDS

Localization of crop damage, gas sensor network, smart farming, biofuel and sorghum.

INTRODUCTION

The production of biofuel energy has become a global trend due to concerns about the traditional fossil fuel sources that generate 34 billion tons of CO_2 every year [1]. Meanwhile, the clean energy sources such as biofuels accounted for only 11% of the total energy production [2]. Despite the advantages of biofuels in environmental aspect, the production of biofuel crops has been limited mainly due to high production costs [3,4]. The current estimated production cost of bioethanol, taking into account the energy per gallon, is approximately 30% higher than that of gasoline [5,6]. Thus, it is critical to lower the biofuel production cost further to facilitate the energy source replacements. To solve the biofuel production cost issue, a smart-farming utilizing advanced technologies such as the gas sensor network is required to reduce the production cost of biofuels as low as the fossil fuels.

Under traditional farm-managements up to 30% of crops are being lost largely due to delayed discovery of insects, weeds or diseases. It is estimated that such a loss corresponds to \$120~360 million loss per year in sorghum production, one of the major biofuel and carbon-sequestration crops in the U.S. [7,8]. This would result in potential loss of bioethanol production, which in turn could demand fossil fuel amounts that would produce an annual emission of 2-6 million CO_2 tons [9,10]. Clearly, improving crop management practices is needed to reduce crop losses and promote sustainable energy production.

To improve traditional farm-managements, some technologies were recently developed and adopted, including imaging from satellites or mobile robot/drones, and insect-capturing containers. However, they have failed to providing either 24-hour continuous monitoring or large monitoring area [11-19]. Specifically, the image-based monitoring system has a limited resolution indicating that a small change during the early stages of herbivore attacks would not be identified. The mobile platform-based monitoring system may not provide comprehensive results, as the monitoring frequency per day is limited. Additionally, the insect-capturing container needs to be replaced regularly.

To overcome these limitations of recent development, our group has developed a real-time, on-site crop stress measurement system [20-27]. Specifically, it developed a wake-up-based gas sensor for long-term field deployment with wireless tethering. However, the developed sensors have not been deployed in a networked configuration and thus not tested for actual field surveillance capabilities yet.

This paper reports the initial deployment of wake-up gas sensors in network and their use to demonstrate the localization capability for plant damage detection in an actual sorghum field in Nebraska. Specifically, it explains the methodology and results of the grid size of a network and localization testing in the field.

METHODOLOGY

Gas Sensor Description

The wake-up sensor was fabricated following the

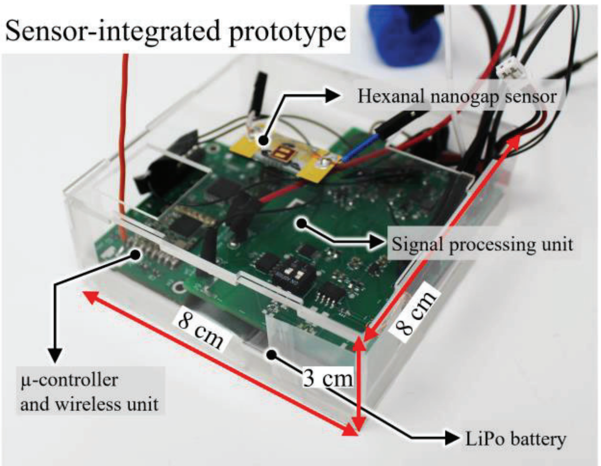

Fig 1. Overview of the integrated prototype integrated with the hexanal nanogap sensor

identical procedures described in the previous papers [20-27]. The nano-gap sensor generated an electrical current upon the capture of a target VOC of hexanal, thus waking-up. The nanogap-based sensor utilized a 5.2-nm gap that was coated with custom-designed linker molecules to selectively capture only hexanal molecules. The capture of a target molecule resulted in a switch-like action in producing electrical current.

Prototype Assembly and Operation

A prototype was assembled by integrating the developed nanogap gas sensor with off-the-shelf interface electronics (a transimpedance amplifier and a comparator), a microcontroller unit, and a LoRa wireless module, as shown in Fig.1. The produced current from a nanogap sensor was converted into a voltage signal by the transimpedance amplifier. The voltage signal was then compared to a reference voltage by a comparator. If the voltage signal exceeded the reference value, the comparator turned on the MCU that subsequently activated the wireless alerting modules, allowing it to transmit data.

Determination of Sensor Grid Size

The sensor grid size was determined by monitoring the wake-up signals by placing sensors at three different distances and monitoring the wake-up activities, as shown in Fig. 2. Specifically, three integrated sensor prototypes were placed at 3, 7, and 10 meters away from the cutting origin, and sorghum leaves were cut at a rate of 50 cuts·min^{-1} continuously for 60 minutes. The sensor signals were monitored for an additional 90 minutes until all the turned-on sensors became turned off naturally.

In parallel, actual gas samples were collected in the field. These gas samples were later analyzed to estimate the concentrations at the moment of measurement in the field and used to validate the grid size monitoring results. For gas collection, standard sample collectors of a sorbent tube (XAD-2, SKC) and SKC pocket touch pump were utilized. They were deployed at distances of 0, 3, 7 and 10 m away from the plant damage location and at different time points of 0, 30 and 60 minutes. The micropump flowed air samples into the sample collectors at a speed of 25 ml·min^{-1} for 16 minutes, resulting in a volume of 400 ml each. The collected gas samples were, then, analyzed in quantities following the already established GC-MS protocol [13]. The quantified gas concentrations, based on GC-MS peak heights, were translated to potential wake-up detection of each sensor at various distances. The translated wake-ups, in terms of timing, were compared to the actual wake-up data from the deployed sensors. Note that, the humidity, temperature and wind speed/direction were monitored and recorded every 30 min at the weather station nearby in the field.

Identification of Localized Plant Damage

Localization testing was conducted using a 2×3 array of prototypes and actual sorghums in the field. 6 prototypes were placed in the array at a 7-meter inter-distance following the determined grid size. As a result, an area of 14×21 m^2 of sorghum was monitored. Each sensor was assigned with an identification number ranging from 1 to 6. A random spot in the lower grid was selected as the cutting area for the sorghums, which is represented by red arrows between purple dots in Fig.5. Cutting was performed following the points from 1 and 2 to 3. The cutting process lasted 60 minutes at a constant speed of 50 cuts/min. Upon initiating the cutting, the wake-up signals from all sensors were monitored. Whenever the detection output exceeded a threshold point, the sensor prototype wirelessly sent an alert to the database. The gas sampling methodology and analysis remained identical to the description provided in the previous section.

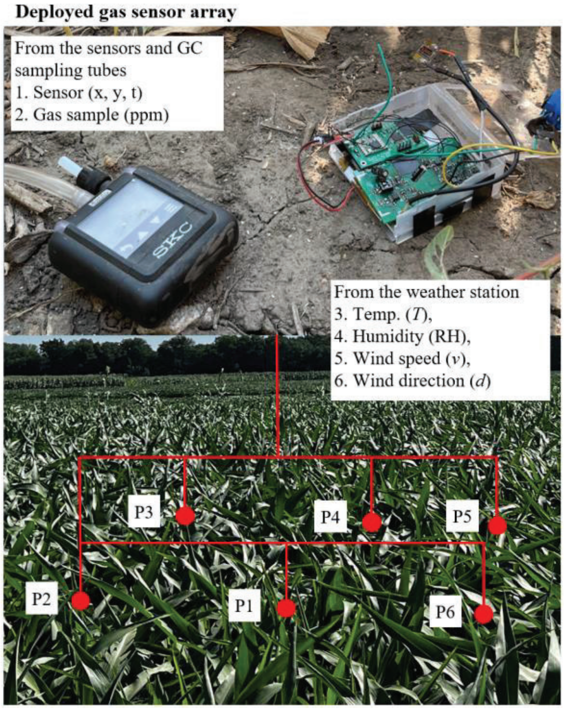

Fig 2. Deployment of gas sensor array, thermometer, hygrometer, and anemometer for the localization testing

RESULTS

Integrated Prototype

The prototype was successfully assembled, combining 1) a nanogap sensor, 2) an amplifier, 3) a comparator, 4) a power generator, 5) a wireless communication unit and 6) a 2000mAh LiPo battery. The prototype held a volume of 3×8×8 cm^3 as shown in Fig. 2. It demonstrated successful performance during the in-lab testing in terms of gas detection, wake-up function and wireless alerting. Then, they were deployed in the field testing.

Determined Grid Size

The grid size for monitoring actual hexanal was determined to be 7 meters, as shown in Fig. 3. The figure shows that the sensor at 3 meters woke up at 14 minutes and the wake-up signal lasted until 63 minutes. Similarly, the sensor at 7 meters woke up at 23 minutes and the wake-up signal lasted until 80 minutes. This indicates that actual hexanal above the threshold concentration was detected at 3 meters and 7 meters at 14 minutes and 23 minutes, respectively, and the sensors were naturally recovered. On the other hand, the sensor located 10 meters away didn't respond during the entire testing period.

The validation of grid size testing was confirmed by analyzing the collected gas samples, as shown in Fig. 4.

The field gas concentrations at the 30-minute point after plant cutting (blue bars) exceeded the threshold concentrations at 0 and 3 meters, matching the wake-up detections of the deployed sensors. Moreover, the field gas concentrations at the 60-minute point after plant cutting (orange bars) exceeded the threshold concentrations at 0, 3, and 7 meters, also matching the corresponding wake-up detections of the deployed sensors. Note that that the predetermined sensor wake-up threshold was 30 ppm, the wind speed was measured as 0~3 mph, the temperature was 41 °C and the humidity was 50% RH.

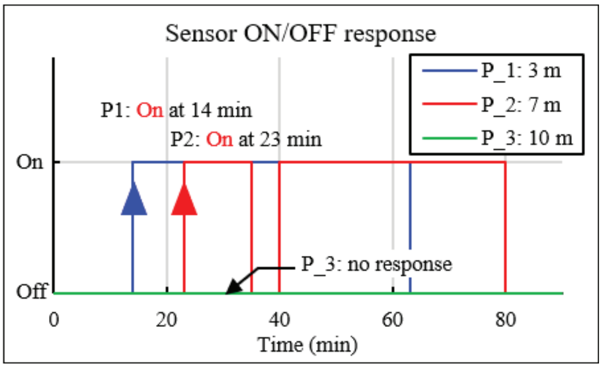

Fig 3. The grid size testing showed the hexanal nanogap sensor can detect the actual hexanal in the grid size of maximum 7-meter radius.

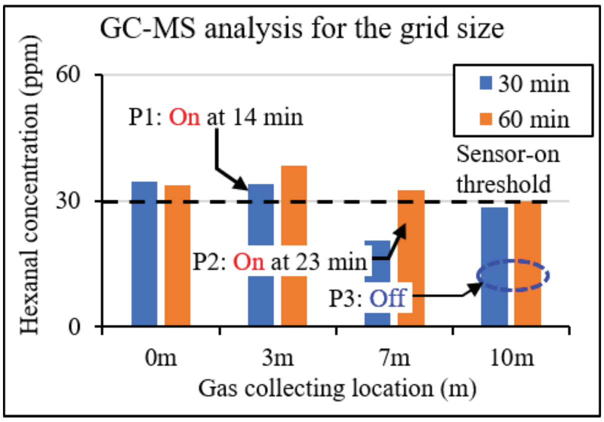

Fig 4. The GC-MS analysis proved the grid-size determination of 7-meter radius.

Identified Location of the Plant Damage

The initial localization capability of the developed sensor network has been successfully demonstrated. The location of damage was identified with 86% reduced area compared to a single sensor-based localization, as shown in Fig. 5. The figure shows an actual field view captured by a drone and the calculated hexanal concentration lines spreading out from the origin at different time points of 43, 64, and 72 minutes with a progression direction towards 95-180° due to the wind. As the hexanal spread out, it triggered the sensor prototypes at various times. The first sensor node P4 was activated at 45 minutes, followed by the sensor node P5 at 62 minutes, and finally, the sensor node P6 at 72 minutes. The other P1, P2, and P3 sensors remained off throughout the entire measurement period.

The measurement data from the sensors was utilized to calculate the timing and location of the progression of 30 ppm hexanal concentration using a custom-developed algorithm. Based on this calculation, the potential damage area was identified and outlined by the green line. The narrowed area was estimated to be 21.7 m^2, which occupied only 7.4% of the total area of 294 m^2. This result suggested that only a small amount of pesticides would be necessary to eliminate the herbivore attacks, and that the other losses of sorghum due to over-sprayed pesticides could be kept, and further potential sorghum damage due to the damage spread could be prevented.

The actual hexanal concentration obtained through GC-MS analysis supported the observations from the sensor measurement data. The comparisons between the actual field hexanal concentrations and the sensor wake-ups at each sensor position are illustrated in Figure 5 and 6, providing clear evidence of a match. The P4 sensor was activated at 45 minutes, and the GC-MS results at the spot at 40 minutes showed a hexanal concentration above 30 ppm. Similarly, the P5 sensor was triggered at 62 minutes,

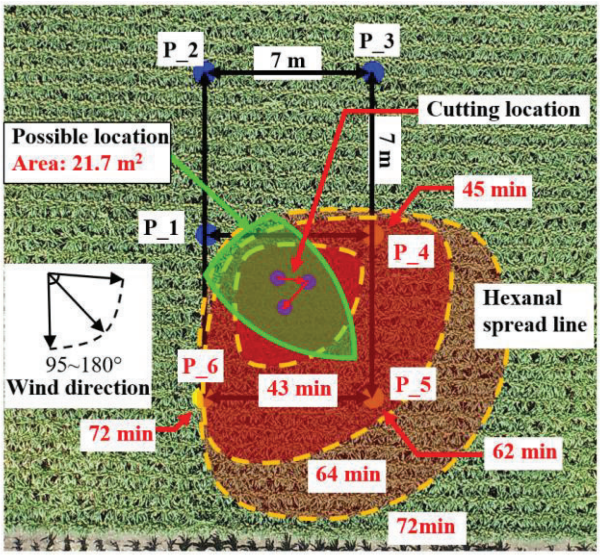

Fig 5. The location testing demonstrated the identification capability of the gas sensor by combining serial turning-on during the actual hexanal spreads overtime.

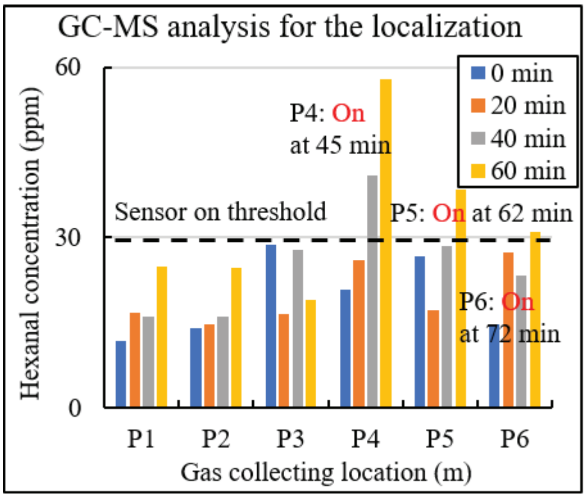

Fig 6. The GC-MS analysis proved the hexanal concentration at the locations of P4, P5, and P6 sensors exceeded the threshold concentration and their turning-on sequence.

and the GC-MS results at 60 minutes showed an above-threshold concentration. At 72 minutes, the P6 sensor was activated, and the GC-MS results indicated that the field concentrations had reached the threshold point at 60 minutes. On the other hand, the GC-MS results also indicated that the field gas concentrations remained below the threshold throughout the entire testing period, which was consistent with the responses from the P1, P2, and P3 sensors during the testing.

CONCLUSION

This paper reports the initial demonstration of the localization capability of the developed nanogap sensors and its network in an actual field setting. The prototype, integrated with the nanogap sensor, was successfully developed and deployed in the sorghum field, where it detected hexanal molecules released from damaged sorghum leaves and transmitted the detection signal to users during the field testing. The detection grid size was determined as a 7-meter radius, and it was confirmed by actual hexanal gas analysis using the established GC-MS protocol. The potential area of the damaged sorghum was identified as 21.7 m^2, occupying only 7.4% of the entire monitoring area, using the monitored sensor network data generated by the deployed 2×3 sensor array. The localized area was 86% smaller compared to single-sensor based localization (153.9 m^2). Thus, it was concluded that the location and timing of sorghum damages caused by mechanical damages can be identified when a network of a gas sensor array is deployed in the field.

ACKNOWLEDGEMENTS

This research work was generously supported by the cooperative agreement of DE-AR0001064 of the ARPAE OPEN 2018 program (Program Manager: Drs. Olga Spahn and David Babson). Microfabrication was performed at the Utah Nanofabrication Facility at the University of Utah.

REFERENCES

[1]. Carbon Dioxide Emissions From Electricity, World Nuclear Association, 2022

[2]. Key World Energy Statistics 2020-Analysis, International Energy Agency, 2020

[3]. Fuel Price Report, Department of Energy, 2023

[4]. C. Obiora, "Optimal Cost of Production of Bioethanol: A Review," 2022, SSRN, pp. 1-13

[5]. Steve Amosson et al., Economic Analysis of Sweet Sorghum for Biofuels Production in the Texas High Plains, Agri-Life extension, 2010

[6]. Ethanol Benefits and Considerations, DOE

[7]. Crop Production Annual Summary, 2021, National Ag Statistical Service (NASS), USDA.

[8]. Crop Value Annual Summary, 2021, NASS, USDA.

[9]. U.M. Sainju et al., "Carbon accumulation in cotton, sorghum, and underlying soil as influenced by tillage, cover crops, and nitrogen fertilization," Plant Soil, 2005, 273, pp.219–234

[10]. R.A.Y. Holou and V. M. Kindomihou, "The Biofuel Crops in Global Warming Challenge: Carbon Capture by Corn, Sweet Sorghum and Switchgrass Biomass Grown for Biofuel Production in the USA," Frontiers in Bioenergy and Biofuels, 2017

[11]. Y. Inoue, "Satellite- and drone-based remote sensing of crops and soils for smart farming – a review," Soil Sci. Plant Nutr., 2020, 66:6, pp. 798-810

[12]. Frank Tenkorang and James Lowenberg-DoBoer, "On-Farm Profitability of Remote Sensing in Agriculture," JTO, 2008, 1:1, pp.50-59.

[13]. G. Sain et al., "Costs and benefits of climate-smart agriculture: The case of the Dry Corridor in Guatemala," Agric. Syst., 2017, 151, pp.163-173

[14]. M. Saqib et al., "A Low-Cost Information Monitoring System for Smart Farming Applications," Sensors, 2020, 20:8, 2367

[15]. P. Prince et al., "Deploying Acoustic Detection Algorithms on Low-Cost, Open-Source Acoustic Sensors for Environmental Monitoring," Sensors, 2019; 19(3):553.

[16]. O. López et al., "Monitoring Pest Insect Traps by Means of Low-Power Image Sensor Technologies," Sensors. 2012; 12(11):15801-15819.

[17]. G. Messina and G. Modica, "Applications of UAV Thermal Imagery in Precision Agriculture: State of the Art and Future Research Outlook," Remote Sensing, 2020; 12(9):1491.

[18]. L. Mei et al., "Agricultural pest monitoring using fluorescence lidar techniques," Appl. Phys. B, 2012, 106, pp.733–740

[19]. F. Martinelli, et al., "Advanced methods of plant disease detection," A review. Agron. Sustain. Dev., 2015, 35, pp.1–25

[20]. S. H. Khan et al., "Detection of a plant signature gas utilizing nano-gap conductivity sensor," MEMS Conference, 2021

[21]. S. H. Khan et al., "Development of a gas sensor for green leaf volatile detection," Transducers Conference, 2021

[22]. S. H. Khan et al., "Field deployment of a nanogap gas sensor for crop damage detection," MEMS Conference, 2022

[23]. S. H. Khan et al., "Field deployment of a nanogap gas sensor for crop damage detection," MEMS Conference, 2022

[24]. S. H. Khan et al., "Early detection of simulated herbivore attacks in sorghum fields through the deployment of very-low-power gas sensor network," Hilton Head Conference, 2022

[25]. S. H. Khan et al., "Characterization of a Wake-Up Nano-Gap Gas Sensor for Ultra Low Power Operation," JMEMS, 2022, 31:5, pp. 791-801

[26]. F. Sium et al., "Theoretical and experimental validation on the tuning capability of the percolation-based in a grid of sensors operation," Hilton Head Conference, 2022

[27]. F. Sium et al., "Ultra-low power gas sensor based on a 3d array of nanogaps," PowerMEMS Conference, 2022

CONTACT

*H. Kim, tel: +1-801-587-9497; hanseup@ece.utah.edu